International Journal of Mechanical, Industrial and Aerospace Sciences
ISSN: 2517-9950
Vol:9, No:1, 2015

A Study on the Comparison of Mechanical and Thermal Properties According to Laminated Orientation of CFRP through Bending Test

Hee Jae Shin, Lee Ku Kwac, In Pyo Cha, Min Sang Lee, Hyun Kyung Yoon, Hong Gun Kim

***Abstract*—**In rapid industrial development, the demand for high-strength and lightweight materials have been increased. Thus, various CFRP (Carbon Fiber Reinforced Plastics) with composite materials are being used. The design variables of CFRP are its lamination direction, order and thickness. Thus, the hardness and strength of CFRP depends much on their design variables. In this paper, the lamination direction of CFRP was used to produce a symmetrical ply [0°/0°, -15°/+15°, -30°/+30°, -45°/+45°, -60°/+60°, -75°/+75° and 90°/90°] and an asymmetrical ply [0°/15°, 0°/30°, 0°/45°, 0°/60° 0°/75° and 0°/90°]. The bending flexure stress of the CFRP specimen was evaluated through a bending test. Its thermal property was measured using an infrared camera. The symmetrical specimen and the asymmetrical specimen were analyzed. The results showed that the asymmetrical specimen increased the bending loads according to the increase in the orientation angle; and from 0°, the symmetrical specimen showed a tendency opposite the asymmetrical tendency because the tensile force of fiber differs at the vertical direction of its load. Also, the infrared camera showed that the thermal property had a trend similar to that of the mechanical properties.

***Keywords*—**Carbon Fiber Reinforced Plastic (CFRP), Bending Test, Infrared Camera, Composite.

I. Introduction

WITH its dimensional stability, material consistency, high strength and stiffness, carbon-fiber reinforced plastic is used across various industries including space, aerospace, sport and leisure as well as for other generic purposes such as structural member and parts, thanks to vigorous research activities and resulting price reduction. Its strength and stiffness in parallel with and perpendicular to the woven direction of fiber is markedly different between fiber and base material due to differences in material property. As compared to isotropic materials, carbon fiber reinforced plastic is very difficult to analyze with theoretical expression of stress analysis (strength and stiffness) due to its directional property, making it inevitable for researchers to analyze it with laboratory test. There has been a substantial amount of researches performed on the carbon fiber reinforced plastic with regard to its compressive material property according to stacking angle and thickness of layers [1]-[3]. However, study on its bending property is also required since structural members are subject to both compressive and bending force when they are exposed to external force.

Despite such necessity, not much study has been performed on the implication of bending force [4]. Out of various rupture behaviors, this researcher performed a bending test on two test pieces each with symmetrical and asymmetrical configuration for this study to analyze relationship between mechanical and thermal characteristics of carbon fiber reinforced plastic with different orientation angle.

H. J. Shin, I. P. Cha, and M. S. Lee are with Department of Mechanical Engineering Jeonju University, 303 Cheonjam-ro, Wansan-gu, Jeonju, 560-759, Korea (e-mail: ostrichs@naver.com, chainpyo007@nate.com, lovely-lms@hanmail.net, respectively).

L. K. Kwac and H. K. Yoon are with Department of Carbon and Nano Engineering Jeonju University, 303 Cheonjam-ro, Wansan-gu, Jeonju, 560-759, Korea (e-mail: kwac29@jj.ac.kr, iylovehk@naver.com, respectively).

H. G. Kim is with Department of Mechanical and Automotive Engineering Jeonju University, 303 Cheonjam-ro, Wansan-gu, Jeonju, 560-759, Korea (corresponding author to provide phone: +82-63-220-2613; fax: +82-63-220-2067; e-mail: hkim@jj.ac.kr)

II. Heat Measurement Theory [5]

It can be shown from classical thermodynamics that the temperature change (Δ T) n an elastic solid subjected to a stress change is given by

$$\Delta T = \frac{T}{\rho C_e} \frac{\partial \sigma_i}{\partial T} + \frac{Q}{\rho C_\varepsilon} \quad (1)$$

where T is the absolute temperature, C_e is the specific heat at constant strain, Q is the heat input, ρ is the mass density, σ_i is the stress change tensor and ε_i is the strain change tensor.

For an isotropic material, with temperature independent material properties, loaded under adiabatic conditions (i.e. Q = 0) (1) can be developed to give

$$\Delta T = -K\, T \quad \sigma_i \quad (2)$$

where K (= $\alpha/\rho C_P$) is a material constant (the "thermoelastic constant" of the material) α is the coefficient of thermal expansion, C_P is the specific heat at constant pressure.

Order of magnitude estimates from (2) indicate that for working stress values in typical engineering materials the temperature change will be of the order 0.01-0.1°C. Infrared radiometry provides the only satisfactory means of monitoring such changes with the required accuracy.

Suppose that a linear infrared detecting system is used to measure Δ T, and that the infrared flux emitted from the surface of the stressed body produces a signal S in the system. Then, if it is assumed that the principal stress normal to the surface of the body is zero from (2) that

$$\sigma_x + \sigma_y = AS \quad (3)$$

where x and y are any pair of orthogonal Cartesian axes in the plane of the emitting surface and A is a "calibration factor" relating the detector signal S to the change in the first invariant of the surface stresses $(\sigma_x + \sigma_y)$.

Equation (3) is the basic "working equation" for quantitative thermoelasitc stress studies with isotropic materials.

Techniques for the determination of the calibration factor A have been reviewed.

Equation (1) can be developed for an orthotropic elastic material by using the appropriate stress-strain-temperature relationship. In such a case the relationship between the temperature change and the stress change becomes

$$\Delta T = -(T/\rho C_P) \quad \alpha_i \sigma_i \quad (4)$$

where α_i are the principal coefficients of thermal expansion of the material and σ_i are the corresponding normal stresses in the principal material directions.

Using (4) in place of (2), the relationship between the thermoelastic signal S and the surface stresses becomes.

$$\alpha_1 \sigma_1 + \alpha_2 \sigma_2 = AS \quad (5)$$

where α_1 and α_2 are the principal coefficients of thermal expansion in the plane of the emitting surface, σ_1 and σ_2 are the normal stresses parallel to the principal axes of the material, and A is a "calibration factor." and (5) is the basic "Working Equation" for quantitative thermoelastic stress studies with orthotropic materials

III. Test Method

Width and length of standard test pieces for bending test are specified in Korean Industrial Standards [6], while ASTM specifies the ratio of thickness and support span of test pieces for bending test as 1:16 in general. With regard to some anisotropic composite materials, however, the test jig was configured according to the test method specified in ASTM 790 standard [7], which allows researchers to measure bending coefficient accurately without being affected by shearing strength when calculating bending strength and stiffness; the test pieces were then cut down following the specification (127×12.7×3.2mm) recommended by ASTM D790.

As the mechanical characteristics of carbon fiber reinforced plastic change according to the orientation of stacking angle of layers due to its anisotropic property [7], The composite material used in this study was USN150B (0.146mm thick), which is the unidirectional carbon fiber prepreg of SK chemicals. This prepreg was laminated in 22 plies, and bending test specimens were manufactured with symmetry ply(0°/0°, -15°/+15°,-30°/+30°,-45°/+45°,-90°/+90°) and asymmetry ply(0°/15°, 0°/30°, 0°/45°, 0°/90°) according to ASTM D790. Table I shows the material property of unidirection prepreg USN150B.

TABLE I
Material Property of Unidirection Prepreg USN150B

Thickness [mm]	Fiber Area Wt[g/m^2]	Resin Content[%]	Total Wt [g/m2]
0.146	150	33	244
Tensile Strength [kgf/mm^2]	**Tensile Modulus [kgf/mm^2]**	**Fiber Density [g/m^2]**	**Resin Density [g/cm^2]**
450	24×10^3	1.77	1.2

Two types of test pieces for the bending test, with either symmetrical (0°/0°, -15°/+15°,-30°/+30°,-45°/+45°,90°/90°) or asymmetrical (0°/15°,0°/30°,0°/45°, 0°/90°) angle against the load applied angle of the fabric, were cut from manufactured composite plate in pursuant to ASTM D790-3 [7]. Stacking method and its shape were shown in Figs. 1 and 2.

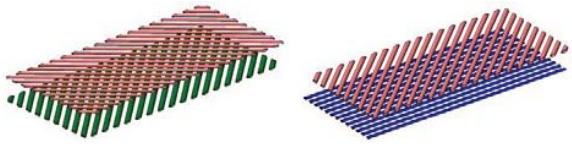

(a) Symmetric specimen (b) Asymmetric specimen

Fig. 1 Stacking Method

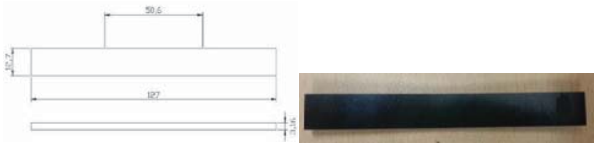

(a) Size of specimen (b) Bending specimen

Fig. 2 CFRP Bending Test Specimen

3-point bending test which is used frequently due to its simplicity and convenience for bending test was adopted for this study as shown in Fig. 3 [4]. Diameter of the support span zig was 10mm in semi-circular form while a nose span zig with 50.6mm span was fixed in the center of the test piece.

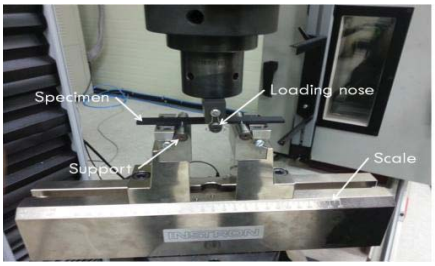

Fig. 3 Installed Specimen for Bending Test

The nose span zig and support span zig were both installed between load cell and actuator on the universal testing machine, while the bending test was conducted by sliding the nose span zig to load applied angle at the speed of 1.350mm/min after placing the test piece on the support span zig. Displacement was controlled within a 5% stain level in pursuant to ASTM 790 [7].

Test conditions were set up by considering required

thickness and size of the test piece as specified by ASTM D709 [7] with details of the test conditions shown in Table II.

At the same time, thermal characteristics of the test piece [8]-[10] were analyzed by measuring its mechanical characteristics and thermal distribution shown on the infrared thermal imaging camera during the bending test.

TABLE II
EXPERIMENT CONDITION FOR BENDING TEST

Support Span [mm]	Cross Head [mm/min]	Depth of Beam [mm]	Deflection [mm]
50.6	1.350	3.16	6.752

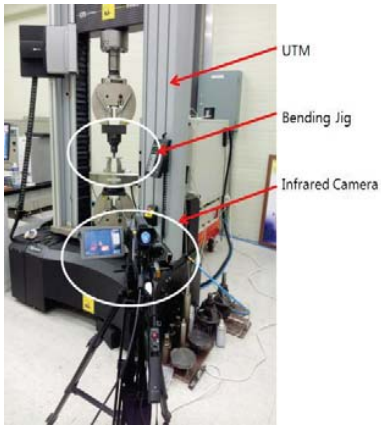

Fig. 4 Bending Test Experiment System

IV. EXPERIMENT RESULTS AND DISCUSSION

Number of test specimens is five specimens for each sample [7]. Test result makes comparison between symmetry and asymmetry by average value of test result. Fig. 5 shows the results of the bending test for symmetry angle.

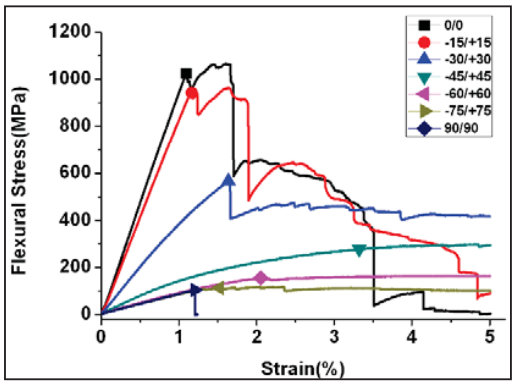

Fig. 5 Symmetry Bending Test result

The strength of the test piece (0°/0°, -15°/+15°, -30°/+30°, 90°/90°) has dropped suddenly as shown in Fig. 5 after it passed the maximum load. The test piece is thought to have been ruptured when it passed the maximum load; the continuous drop of stress level interrupted intermittently at multiple stages is thought be the result of rupture of fiber at each stage; unlike other test pieces with rapidly increasing loads, those test pieces each with (-45°/+45°, -60°/+60°, -75°/+75°) stacking angle saw their load increase rather slowly before they snapped eventually. This is thought to have been caused by the continuous bending of the test pieces under low load before the onset of slack without rupture when some smaller rupture occurred at the outermost corner of the test piece. The test piece with a -90°/+90° stacking angle is thought to have been ruptured by a very slight load since the length of fiber aligns with the load applied angle.

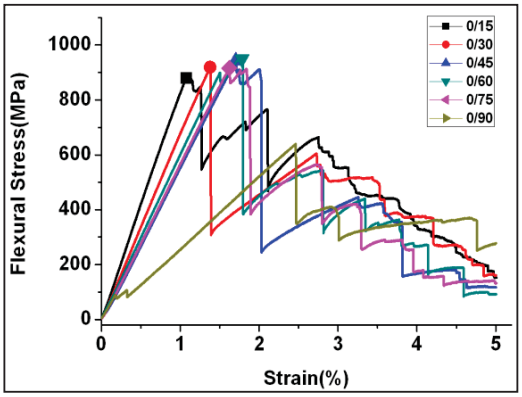

Fig. 6 Asymmetry Bending Test Result

Fig. 6 shows the load-elongation graph of the test pieces measured after the bending test according to the change of stacking angle with asymmetrical fiber configuration. As shown in Fig. 8, all of those test pieces each with (0°/15°, 0/30°, 0/45°, 0/60°, 0/75°, 0/90°) stacking angle saw their load decrease markedly past the inflection point at maximum load, which is thought to have been caused by the same mechanism observed in the rupture of fiber with symmetrical configuration.

Fig. 7 is relation between max flexural stress and Lamination angle for bending test. Meanwhile the bending test with symmetrical configuration in Fig. 7 shows that the test pieces with 0°/0° stacking angle demonstrated the highest bending strength. However, the higher the fiber ply orientation rises, the weaker the bending strength has become, with lowest bending strength observed in the test pieces with a 90°/90° stacking angle, which may prove that given the carbon fiber reinforced plastic with the same material composition, its load applied angle changes according to its respective fiber ply orientation. The test result of the test pieces with asymmetrical configuration shows that their bending strength has risen with the increase of fiber ply orientation but it went down with 0°/90° stacking angle, which may prove that its bending strength has decreased since the load applied angle of the nose aligns with its fiber ply orientation.

To analyze the thermal distribution of carbon fiber reinforced plastic composite material during the bending test, its thermal distribution has been measured up until the rupturing point of the test pieces.

Fig. 8 shows that the thermal difference was measured by averaging the initial temperature and the temperature at the moment of rupture while the area of initial rupturing point was

represented as one side (area01).

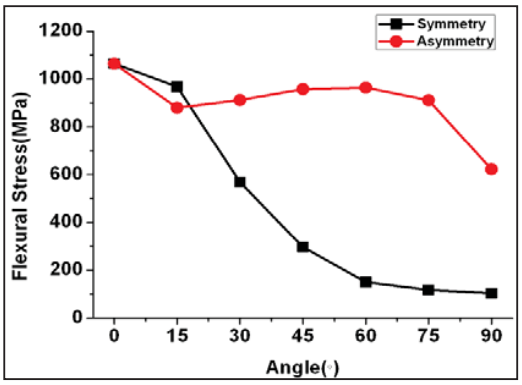

Fig. 7 Bending Test Relation between Max Flexural Stress and Lamination Angle

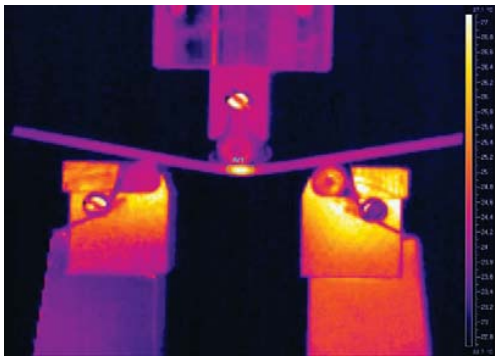

Fig. 8 Temperature Distribution of Bending Test

Fig. 9 (a) shows the result of the bending test on carbon fiber reinforced plastic samples along their thermal distribution which was performed according to their ply orientation and captured by infrared thermal imaging camera: the average temperature has slid down with the rise of the fiber ply orientation past the -15°/+15° stacking angle.

Fig. 9 (b) shows that the increase of fiber ply orientation coincided with the rising average temperature of its rupture surface: the energy generated during the rupture of the test piece in a very short time is thought to have been emitted as high heat, since its load applied angle aligns with its fiber ply orientation in the rapidly up-sloping zone in the graph.

V. Conclusion

It is believed that the load has dropped sporadically along multiple stages in the symmetrical and asymmetrical graph because of the rupture of fiber at each different stage; unlike other test pieces with rapidly increasing load, those test pieces saw their load increase rather slowly before they snapped eventually. This is thought to have been caused by the continuous bending of the test piece under low load before an onset of slack without a rupture when some smaller rupture occurred at the outermost corner of the test piece.

In the test conducted on test pieces with asymmetrical configuration, their bending load rose with the increase of fiber ply orientation, while in the test with symmetrical configuration, the bending load dropped with the rise of fiber ply orientation past the point of 0° stacking angle; unlike as in the asymmetrical, it is believed to have been caused by the fiber's lack of tensile strength along the length of fiber with symmetrical configuration; and with regard to the load applied on the nose span zig, the load is believed to have decreased not so much by the inherent weakness of the fiber as the rupture itself.

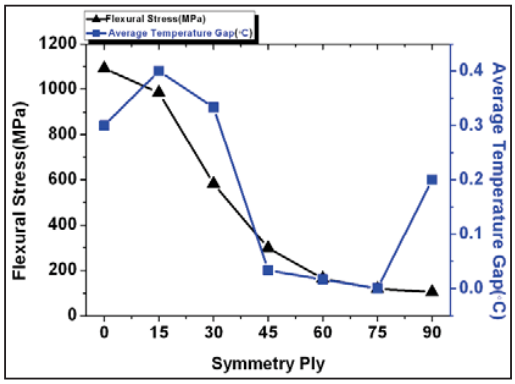

(a) Symmetry Ply

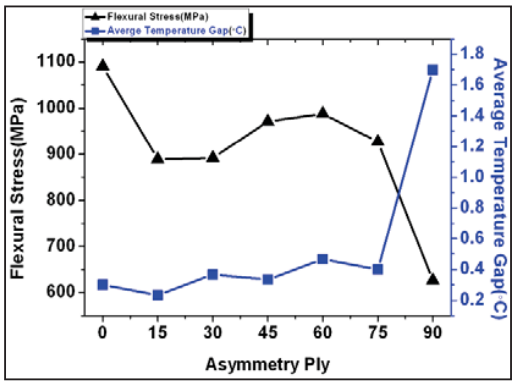

(b) Asymmetry Ply

Fig. 9 of Bending Test Relation between Temperature Difference and Max Flexural Stress

The thermal distribution of the carbon fiber reinforced plastic test pieces with symmetrical configuration started to decrease beginning at -15°/+15° stacking angle while it increased with the rise of fiber ply orientation in the test pieces with asymmetrical configuration, which follows a similar trend shown in the bending load graph according to its fiber ply orientation. From such observations it can be concluded that the average temperature would rise when the fiber, when placed along the length, endure the bending load, while the energy generated from the rupture of fiber within a short time is believed to have dissipated as high heat.

ACKNOWLEDGMENT

This research was supported by the Ministry of Education, Science Technology (MEST) and National Research Foundation of Korea (NRF) through the Human Resource Training Project for Regional Innovation (No. 2012H1B8A2026147) and financially supported by basic science research program through the national research foundation of Korea (NRF) funded by the ministry of education, science and technology (No. 2013R1A1A2061581)

REFERENCES

[1] J. H. Kim, I. Y. Yang and J. K. Sim, "Evaluation of Fracture Toughness of Dynamic Interlaminar for CFRP Laminate Plates by Resin Content," KSMTE, Vol. 12, No. 4, pp. 43-49, 2003.
[2] K. H. Kim, N. S. Park, S. W. Ra, Y. N. Kim, H. Lee, J. K. Sim and I. Y. Yang, "Characteristics of Low Velocity Impact Responses due to Interface Number and Stacking Sequences of CFRP Composite Plates," KSMTE, Vol. 10,No. 6, pp. 48~56, 2001.
[3] Y. N. Kim, K. H. Im, J. W. Park and I. Y. Yang, "Experimental approach on the collapse mechanism of CERP composite tube," Reviews of progress in QNDE, pp. 95-99, 2000.
[4] I. Y. Yang, J. H. Kim, J. K. Sim and J. H. Kim, "Evaluation of Characteristics of CFRP Structural member's Bending Strength and Rigidity," KSMTE, pp. 556~560, 2008.
[5] P. Stanley, " Applications and potential of thermoelastic stress analysis" Achievements in Mechanical and Materials Engineering, Vol. 64, Issues1-3, PP. 359-370, February 1997
[6] Determination of Flexural Properties of Rigid Plastics, KS M 3008.
[7] Standard Test Methods for Flexural Properties of Unreinforced and Reinforced Plastics and Electrical Insulating Materials, ASTM, D790-03.
[8] M. Y. Choi and W. T. Kim, "The Utilization of Nondestructive Testing and Defects Diagnosis using Infrared Thermography," The Korean Society for Nondestructive Testing, Vol. 24, No. 5, pp. 525-531, 2004.
[9] W. T. Kim, M. Y. Choi, H. w. Park, and Y. K. Han, "Thermography Patterns and Temperature Profiles of Blocks with Internal Defects," KSNT/SC0022, pp. 14-15, 2004.
[10] J. Y. Kim, D. J. Yang, J. H. Han, S. You, C. H. Kim, and K. S. Song, "The Development of Automatic Detection Monitoring System for Thermal Failure Part by Infrared Thermal Vision Camera," KSNT/SC0038, pp. 14-15, 2004.